Adsorption of EDTA on activated carbon from aqueous solutions

Hai-song Zhu, Xiao-juan Yang, Yan-peng Mao, Yu Chen, Xiang-li Long*, Wei-kang Yuan

State Key Laboratory of Chemical Engineering, East China University of Science and Technology, Meilong Road 130, Shanghai 200237, People's Republic of China

ARTICLE INFO

ABSTRACT

In this study, the adsorption of EDTA on activated carbon from aqueous solutions has been investigated in a batch stirred cell. Experiments have been carried out to investigate the effects of temperature, EDTA concentration, pH, activated carbon mass and particle size on EDTA adsorption. The experimental results manifest that the EDTA adsorption rate increases with its concentration in the aqueous solutions. EDTA adsorption also increases with temperature. The EDTA removal from the solution increases as activated carbon mass increases. The Langmuir and Freundlich equilibrium isotherm models are found to provide a good fitting of the adsorption data, with $R^2 = 0.9920$ and 0.9982, respectively. The kinetic study shows that EDTA adsorption on the activated carbon is in good compliance with the pseudo-second-order kinetic model. The thermodynamic parameters (E_a, ΔG^0, ΔH^0, ΔS^0) obtained indicate the endothermic nature of EDTA adsorption on activated carbon.

© 2010 Elsevier B.V. All rights reserved.

1. Introduction

Power plant flue gas frequently contains NO_x and SO_2 pollutants that cause acid rain and urban smog. The approach that adds iron(II)(EDTA) (EDTA, ethylenediaminetetraacetate) into the scrubbing liquor to promote the solubility of NO via formation of iron(II)(EDTA)NO has been researched extensively [1–5]. Although Fe^{II}–EDTA can obtain a high NO removal efficiency, it is easily oxidized to Fe^{III}–EDTA that is not capable of binding NO [6,7]. Many methods [8–11] have been put forward to regenerate Fe^{II}–EDTA to sustain the NO removal efficiency. The authors [12] put forward to utilize activated carbon as a catalyst to speed up the regeneration of iron(II)(EDTA). Activated carbon is used to catalyze the reduction of Fe^{III}–EDTA to Fe^{II}–EDTA so as to maintain the capability of removing NO from gas streams. According to the mechanism discussed in literature [12], the adsorption of EDTA on activated carbon is an important factor affecting the catalytic reduction of Fe^{III}–EDTA.

Activated carbon is one of the adsorbents used widely for various gas separation and purification processes, owing to its distinguished properties such as extensive pore surface area, developed internal pore structure, and unique surface chemistry. Many authors have studied the adsorption on activated carbons. Long et al. [13] reported that ammonia adsorption on the activated carbons could be well described by the pseudo-second-order kinetic equation. Fletcher et al. [14] investigated the adsorption and desorption kinetics for hydrophilic and hydrophobic vapors on activated carbon. EDTA is a chelating agent widely used in industry and agriculture. For example, Jones et al. [15] studied the interaction of EDTA with barium sulfate. Repo et al. [16] reported their study on the Removal of Co(II) and Ni(II) ions from contaminated water using silica gel functionalized with EDTA and/or DTPA as chelating agents. Detailed metal–EDTA adsorption and EDTA adsorption results have also been reported. Bowers and Huang [17] tested a ligand-type adsorption behavior for several equimolar metal–EDTA complexes onto γ-Al_2O_3. Nowack et al. [18] reported the adsorption of metal–EDTA complexes onto aluminum and iron oxides. Muhammad [19] completed adsorption modeling employing the diffuse layer model considering inner-sphere complex formation between Pb(II), EDTA, Pb(II)–EDTA, and the TiO_2 surface. Furlong et al. [20] reported the adsorption of EDTA onto TiO_2.

However, the thorough investigations of EDTA sorption onto activated carbon are not presented in commonly used literature. In this study, EDTA adsorption on activated carbons from aqueous solutions has been investigated. The kinetic study shows that EDTA adsorption on the activated carbon is in good compliance with the pseudo-second-order kinetic model. The thermodynamic parameters (E_a, ΔG^0, ΔH^0, ΔS^0) obtained indicate the endothermic nature of EDTA adsorption on activated carbon.

2. Experimental

2.1. Experimental set-up

Batch experiments were performed in a stirred glass flask of 500 ml to investigate the EDTA adsorption on activated carbon from aqueous solutions. The schematic

* Corresponding author. Tel.: +86 21 6425 3267; fax: +86 21 6425 3528.
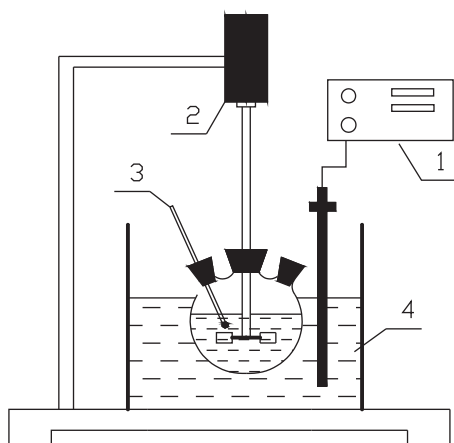*E-mail address:* longdragon@ecust.edu.cn (X.-l. Long).

**Fig. 1.** The schematics of EDTA adsorption performed in a stirred cell reactor. (1) Electric relay, (2) stirrer rod, (3) thermometer and (4) stirred cell.

Fig. 2. Effect of stirring speed on EDTA adsorption (AC = 12.5 g l^{-1}, EDTA = 0.01 mol l^{-1}, pH = 4.35, T = 50 °C).

diagram of the experimental apparatus is shown in Fig. 1.

A turbine impeller with diameter of 3 cm was mounted on the bottom of the stirring rod. Measured amount of Na$_2$H$_2$EDTA was dissolved into distilled water to make up EDTA aqueous solution. Four hundred milliliter EDTA aqueous solution and appropriate dose of activated carbon were introduced into the glass flask.

A commercial activated carbon of coconut shell was used in this experiment. The physicochemical characteristics of the activated carbon of coconut shell are listed in Table 1. The concentration of surface groups on carbons was determined by Boehm titration. The stirring speed was 300 rpm. The initial pH values of EDTA solutions were adjusted to the desired value with NaOH (1.0 mol l^{-1}) solution at 25 °C. The liquid samples were withdrawn periodically to determine the changes of EDTA concentration in the aqueous solution during the experiments.

2.2. Analysis methods

The EDTA concentration was determined by titration with ZnCl$_2$ solution of 0.01 mol l^{-1} using indicator xylenol orange and buffer solution of pH 5.5. Zn^{2+} combine with EDTA as follows:

$$Zn^{2+} + EDTA^{2-} \rightarrow ZnEDTA \tag{1}$$

The titration end point is obtained as the solution turns into Purple-red because Zn–XO chelate is generated by xylenol orange combining with Zn^{2+}:

$$Zn^{2+} + XO \rightarrow Zn\text{–}XO \tag{2}$$

EDTA adsorption (mg g^{-1}) was calculated by using the following equation:

$$q_e = \frac{(C_0 - C_t) \times V \times 291 \times 1000}{m} \tag{3}$$

Table 1
Physicochemical characteristics of the activated carbon of coconut.

Parameter	Value
Bulk density	0.50 g cm^{-3}
pH	9.20
Carbonyl group	0.250 mmol g^{-1}
Lactonic group	0.074 mmol g^{-1}
Hydroxyl group	0.058 mmol g^{-1}
Basic surface functional groups	0.325 mmol g^{-1}
Specific surface area	1050 m^2 g^{-1}
Iodine number	1000 mg g^{-1}
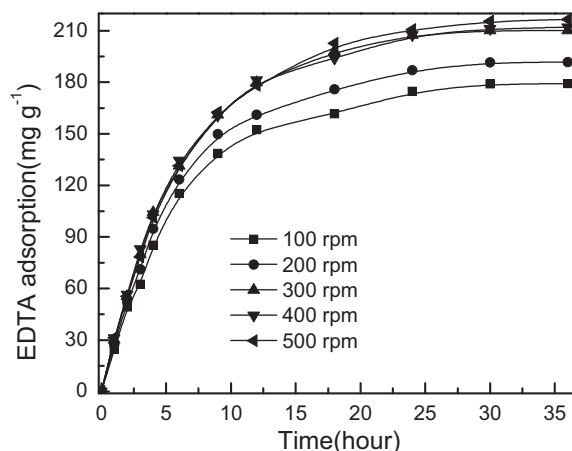
where m is the mass of activated carbon (g), C_0 is the initial EDTA concentration and C_t is the EDTA concentration (mol l^{-1}) at t time in the solution, 291 is the molecular weight of EDTA, and V is the volume of aqueous EDTA solution (l).

3. Results and discussion

3.1. Effect of stirring speed on EDTA adsorption

To investigate the effect of stirring speed on EDTA adsorption, experiments were performed under different stirring speed while keeping other parameters constant. The experimental results obtained are shown in Fig. 2.

Fig. 2 suggests that the equilibrium uptake of EDTA on activated carbon increases from 179 mg g^{-1} to 210 mg g^{-1} as stirring speed increases from 100 r min^{-1} to 300 r min^{-1}. Fig. 2 also depicts that it takes 30 h for the adsorption of EDTA to reach equilibrium. However, the adsorption of EDTA does not increase as the stirring speed increases above 300 r min^{-1}. The reason may be that there is a stagnant flow layer existing on activated carbon surface. Increasing the stirring rate will reduce the thickness of the liquid film and the mass-transfer resistance to the activated carbon surface. Therefore, the adsorption of EDTA on activated carbon will be enhanced with the stirring speed. However, the impact of the external diffusion has been eliminated as the stirring speed increases above 300 r min^{-1}. Hence, the EDTA adsorption may not increase further as the stirring speed rises.

3.2. Effect of activated carbon particle size on EDTA adsorption

The experiments were carried out to investigate the effect of activated carbon particle size on EDTA adsorption. The experimental results obtained are shown in Fig. 3. Fig. 3 depicts that the equilibrium uptake of EDTA on activated carbon increases from 167 mg g^{-1} to 210 mg g^{-1} as the particle decreases from 0–40 mesh to 80–120 mesh. The EDTA adsorption on the activated carbon is not improved further as the particle size decreases below 80–120 mesh. The intragranular diffusion of EDTA on the activated carbon will be enhanced as the activated carbon particle size decreases. Thus, the EDTA adsorption on the activated carbon increases as the particle size decreases. However, the adsorption of EDTA will not be increased further because the impact of internal diffusion has been eliminated as the activated carbon particle decreases below 80–120 mesh.
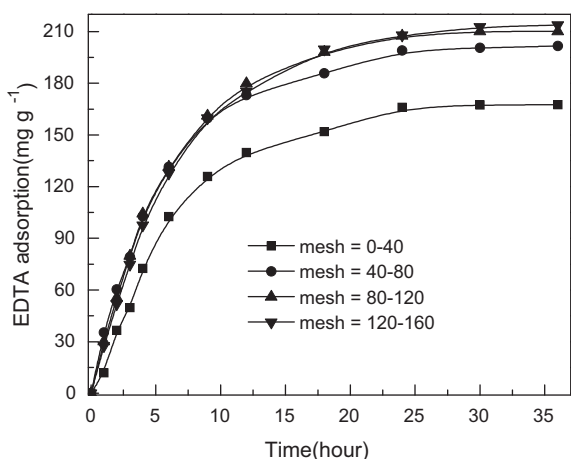
Fig. 3. Effect of mesh of activated carbon on EDTA adsorption (AC = 12.5 g l^{-1}, EDTA = 0.01 mol l^{-1}, pH = 4.35, T = 50 °C, stirring speed = 300 r min^{-1}).

3.3. Effect of temperature on EDTA adsorption

Experiments were carried out at the same initial EDTA concentration of 0.01 mol l^{-1} with an activated carbon dose of 12.5 g l^{-1} to investigate the effect of temperature on EDTA adsorption. The results shown in Fig. 4 illustrate that EDTA adsorption increases with temperature. After 36 h operation, the EDTA adsorption increases from 174 to 261 mg g^{-1} as the temperature increases from 40 °C to 70 °C. The increase in uptake with rise in temperature is due to the fact that the reaction rate between EDTA and the surface oxygen functional groups on the activated carbon increases with temperature. Furthermore, the diffusivity of sorbate through the external laminar layer into the micropores of the adsorbent also increases with temperature as diffusion is an endothermic process. On the other hand, as Terzyk [21] has studied, some water molecules (bonded by strong hydrogen bonds with surface groups located at entrances to pores) can desorb from activated carbon as temperature increases, which results in more pores open to EDTA.

3.4. Effect of EDTA concentration on its adsorption

Experiments have been performed to test the effect of EDTA concentration on its adsorption on activated carbon. The experimental results shown in Fig. 5 suggest that the EDTA adsorption on activated carbon increases with its concentration in the aqueous
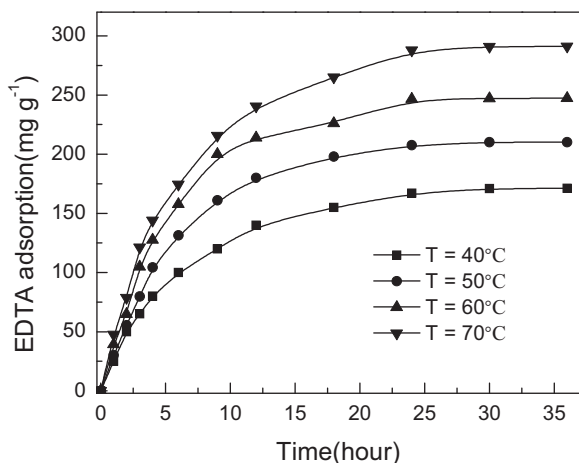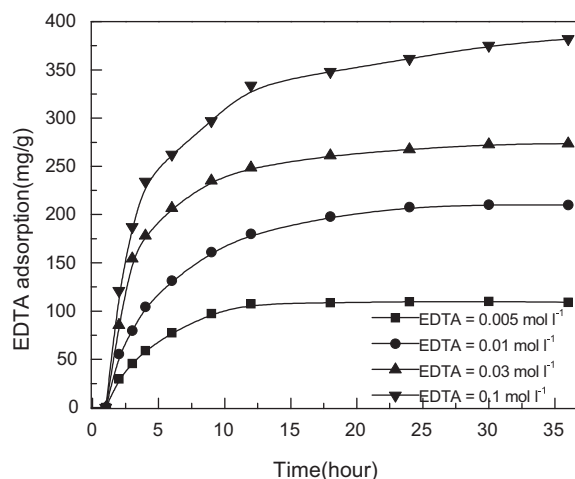

Fig. 5. Effect of concentration on EDTA adsorption (AC = 12.5 g l^{-1}, pH = 4.35, T = 50 °C, stirring speed = 300 r min^{-1}).

solutions. After 36 h operation, the EDTA adsorption on activated carbon is 109 mg g^{-1}, 210 mg g^{-1}, 273 mg g^{-1} and 382 mg g^{-1} for the initial EDTA concentration of 0.005 mol l^{-1}, 0.01 mol l^{-1}, 0.03 mol l^{-1}, 0.1 mol l^{-1}, respectively. The explanation can be expressed as follows. Firstly, the mass-transfer impetus between the liquid bulk and the surface of activated carbon increases with the initial EDTA concentration in the aqueous solution. Secondly, the diffusivity of EDTA also increases with its concentration. Thirdly, the EDTA on the surface of activated carbon in equilibrium with the EDTA in the solution will increase with its concentration in the solution.

3.5. Effect of activated carbon mass on EDTA adsorption

To investigate the effect of activated carbon mass on EDTA adsorption, 0.01 mol l^{-1} EDTA solutions were mixed with different activated carbon mass for 36 h, while keeping other parameters constant. It can be seen from the experimental results depicted in Fig. 6 that EDTA adsorption on per gram of activated carbon decreases as the activated carbon mass in the solution increases. For example, after 6 h operation, the EDTA adsorption decreases from 295.7 to 131.5 mg g^{-1} as activated carbon mass increases from 1.25 g l^{-1} to 12.5 g l^{-1}. Such performance on the adsorbent may be attributed to the fact that some of the adsorption sites remain unsaturated during the adsorption process. As the initial
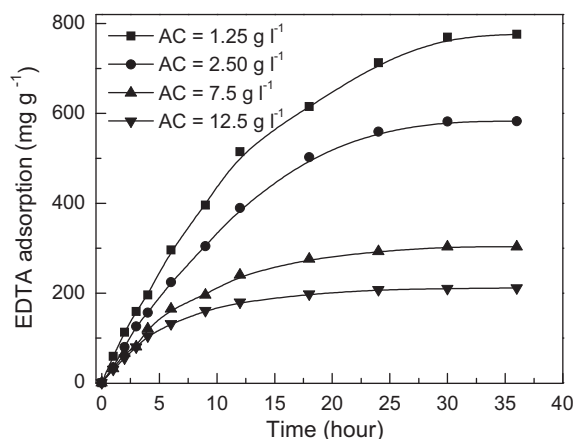

Fig. 4. Effect of temperature on EDTA adsorption (AC = 12.5 g l^{-1}, EDTA = 0.01 mol l^{-1}, pH = 4.35, stirring speed = 300 r min^{-1}).

Fig. 6. Effect of activated carbon mass on EDTA adsorption (EDTA = 0.01 mol l^{-1}, pH = 4.35, T = 50 °C, stirring speed = 300 r min^{-1}).
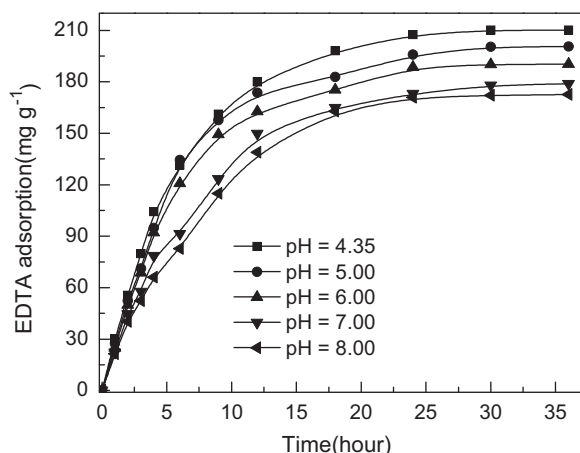
Fig. 7. Effect of pH on EDTA adsorption (AC = 12.5 g l^{-1}, EDTA = 0.01 mol l^{-1}, T = 50 °C, stirring speed = 300 r min^{-1}).

EDTA concentration keeps constant, it is noted that the total adsorptive capability of EDTA increases faster as the activated carbon mass increases because of the increase in the number of reaction sites and surface area available to EDTA. For example, it can be calculated from the experimental results depicted in Fig. 6 that the total EDTA adsorption increases from 370 mg l^{-1} to 1644 mg l^{-1} as activated carbon mass increases from 1.25 g l^{-1} to 12.5 g l^{-1}.

3.6. Effect of pH on EDTA adsorption

Effect of pH on the adsorption of EDTA on activated carbon is shown in Fig. 7. Fig. 7 demonstrates that the pH value on EDTA adsorption cannot be ignored. As pH increases, the equilibrium adsorbate decreases. As the initial pH value increases from 4.35 to 8, the equilibrium adsorbate decreases from 210 mg g^{-1} to 172 mg g^{-1}. The explanation can be expressed as follows. When pH values range from 3 to 10, the main form of EDTA is H_2Y^{2-} or HY^{3-} in the aqueous solution, which is negatively charged. Activated carbon surface has a weak polarity under different pH value. In the acidic conditions, the surface of activated carbon is positively charged, which is favorable for the adsorption of anionic species. As pH rises, the surface of activated carbon gradually becomes negative charged, which may result in the decrease of EDTA adsorption.

3.7. Adsorption dynamics

3.7.1. The pseudo-first-order kinetic model

The pseudo-first-order kinetic model has been widely used to predict adsorption kinetics. A linear form of pseudo-first-order model was described by Lagergren:

$$\ln(q_e - q_t) = \ln q_e - k_1 t \tag{6}$$

where q_t is the amount adsorbed at time t (mg g^{-1}), and k_1 is the rate constant of pseudo-first-order adsorption (h^{-1}). The values of $\ln(q_e - q_t)$ are calculated from the kinetic data (Fig. 4).

The plots of $\ln(q_e - q_t)$ versus t are shown in Fig. 8. The values of k_1 and $\ln q_e$ can be obtained from the slopes and the intercepts of the curves. The calculated q_e, k_1, and the corresponding linear regression correlation coefficient R^2 values are shown in Table 2. The low correlation coefficients show that the pseudo-first-order model does not predict the kinetics of the EDTA adsorption onto activated carbon accurately.
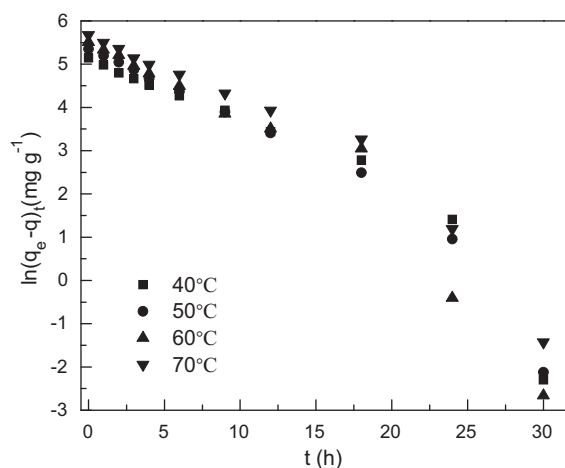

Fig. 8. Lagergren pseudo-first-order kinetics for EDTA adsorption onto activated carbon (AC = 12.5 g l^{-1}, EDTA = 0.01 mol l^{-1}, pH = 4.35, stirring speed = 300 r min^{-1}).

3.7.2. The pseudo-second-order kinetic model

The kinetic data can also be analyzed using Ho and McKay's pseudo-second-order kinetics, represented by [22]

$$\frac{t}{q_t} = \frac{1}{k_2 q_e^2} + \frac{1}{q_e} t \tag{7}$$

where k_2 is the rate constant of second-order adsorption (g mg^{-1} h^{-1}). The values are calculated from the kinetic data (Fig. 4). A plot between t/q_t versus t gives the value of the constants k_2 (g mg^{-1} h^{-1}) and also q_e (mg g^{-1}) can be calculated.

The curves of the plots of t/q_t versus t were given in Fig. 9 and the calculated q_e, k_2, and the corresponding linear regression correlation coefficient R^2 values are summarized in Table 2. The correlation coefficients for the second-order kinetics model (R^2) are greater than 0.99, indicating the applicability of this kinetics equation and the second-order nature of the adsorption process of EDTA onto activated carbon.

3.7.3. Intraparticle diffusion

The adsorbate species are probably transported from the bulk of the solution into the solid-phase through an intraparticle diffusion process, which is often the rate limiting step in many adsorption processes. The possibility of intraparticle diffusion was explored by using the intraparticle diffusion model [23,24]

$$q_t = k_3 t^{1/2} + C \tag{8}$$

Table 2
Kinetic parameters for the adsorption of EDTA on AC at various temperatures.

	40 °C	50 °C	60 °C	70 °C
Pseudo-first-order				
k_1 (min^{-1})	0.20	0.22	0.25	0.21
$q_{e,cal}$ (mg g^{-1})	237.5	281.5	368.7	395.4
q_e (mg/g)	171.1	210.0	247.3	291.0
R^2	0.8973	0.9466	0.9315	0.8700
Pseudo-second-order				
k_2 (g mg^{-1} h^{-1})	8.73E−04	7.84E−04	7.73E−04	5.82E−04
$q_{e,cal}$ (mg g^{-1})	196.1	238.1	270.3	294.1
q_e (mg g^{-1})	171.1	210.0	247.3	291.0
R^2	0.9984	0.9950	0.9939	0.9977
Intraparticle diffusion				
k_3 (mg g^{-1} h$^{-1/2}$)	29.44	36.43	41.57	49.30
$q_{e,cal}$ (mg g^{-1})	194.3	242.9	285.1	329.0
q_e (mg g^{-1})	171.10	210.03	247.3	291.0
C	17.61	24.36	35.65	37.30
R^2	0.9237	0.8849	0.8706	0.9073
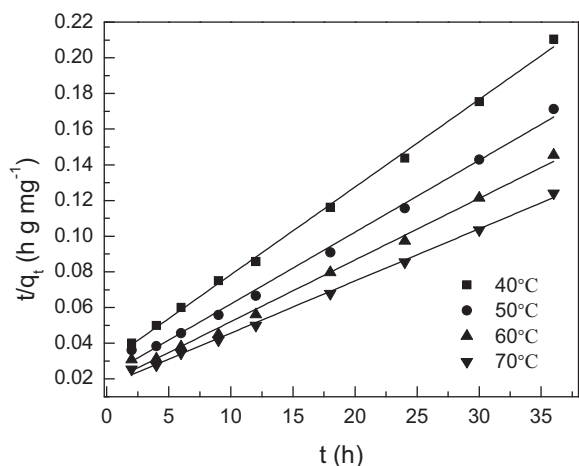
Fig. 9. Ho pseudo-second-order kinetics for EDTA adsorption onto activated carbon ($AC = 12.5\,g\,l^{-1}$, $EDTA = 0.01\,mol\,l^{-1}$, $pH = 4.35$, stirring speed $= 300\,r\,min^{-1}$).

where C is the intercept and k_3 is the intraparticle diffusion rate constant ($mg\,g^{-1}\,h^{-1/2}$). Plots between q_t versus $t^{1/2}$ are given in Fig. 10. The values k_3, C, and the corresponding linear regression correlation coefficient R^2 values are given in Table 2. From Table 2, it is observed that k_3 increases with temperature.

3.8. Adsorption isotherm

3.8.1. Langmuir isotherm

Langmuir equation is based on a theoretical model and assumes that the maximum adsorption corresponds to a monolayer saturated with adsorbate molecules on the adsorbent surface that is energetically homogeneous. Langmuir isotherm constants are calculated from the following linearized form:

$$\frac{C_e}{q_e} = \frac{1}{bQ} + \frac{C_e}{Q} \tag{9}$$

where Q and b are Langmuir constants determined from the slope and intercept of the plot, indicative of maximum adsorption capacity ($mg\,g^{-1}$) of adsorbent and energy of adsorption, respectively, while C_e is the remaining concentration of adsorbate after equilibrium ($mg\,l^{-1}$) and q_e is the amount adsorbed at equilibrium ($mg\,g^{-1}$). From the equilibrium uptake of EDTA shown in Fig. 6, a Langmuir isotherm curve can be given by plotting C_e/q_e against C_e (see Fig. 11). Fig. 11 demonstrates that the adsorption isotherm
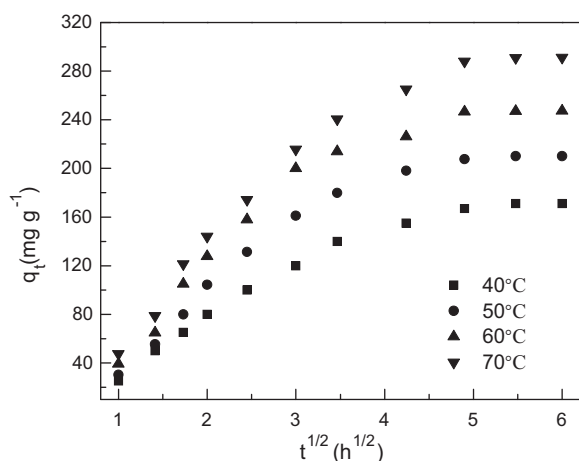

Fig. 10. Intraparticle diffusion plots for EDTA adsorption onto activated carbon ($AC = 5\,g$, $EDTA = 0.01\,mol\,l^{-1}$, $pH = 4.35$, stirring speed $= 300\,r\,min^{-1}$).
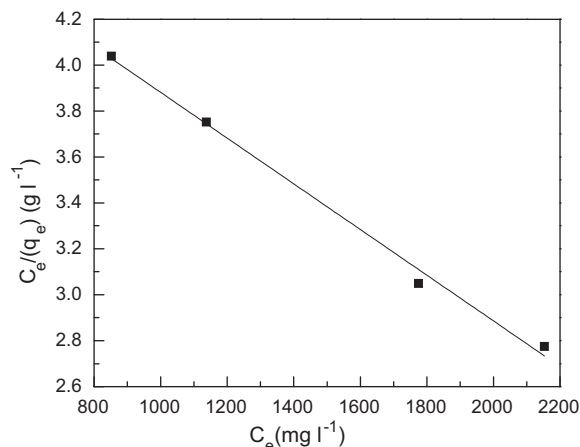
Fig. 11. Langmuir isotherm curve ($EDTA = 0.01\,mol\,l^{-1}$, $pH = 4.35$, $T = 50\,°C$, stirring speed $= 300\,r\,min^{-1}$).

is in good agreement with the Langmuir adsorption equation. The slope is Q^{-1} and the intercept is Q/b. A value of 1005.05 mg g^{-1} is obtained for Q and a value of 206.11 is obtained for b (correlation coefficient 0.9920).

3.8.2. Freundlich isotherm

Freundlich isotherm assumes that the uptake of adsorbate occurs on a heterogeneous surface by multilayer adsorption and that the amount of adsorbate adsorbed increases infinitely with an increase in concentration. The Freundlich isotherm is expressed as:

$$q_e = K \cdot C_e^{1/n} \tag{10}$$

where K and n are constants of Freundlich isotherm incorporating adsorption capacity ($mg\,g^{-1}$) and intensity, while C_e and q_e are the remaining concentration of adsorbate after equilibrium ($mg\,l^{-1}$) and the amount adsorbed at equilibrium ($mg\,g^{-1}$), respectively. Taking logarithm from Eq. (10), a linearized form of Freundlich isotherm can be represented as follows:

$$\log(q_e) = \log K + 1/n \log C_e \tag{11}$$

A Freundlich isotherm curve can be given by plotting $\log(q_e)$ against $\log(C_e)$ (as seen in Fig. 12). In terms of Fig. 12, the Freundlich isotherm can be given as follows ($n = 0.699$, correlation coefficient 0.9983):
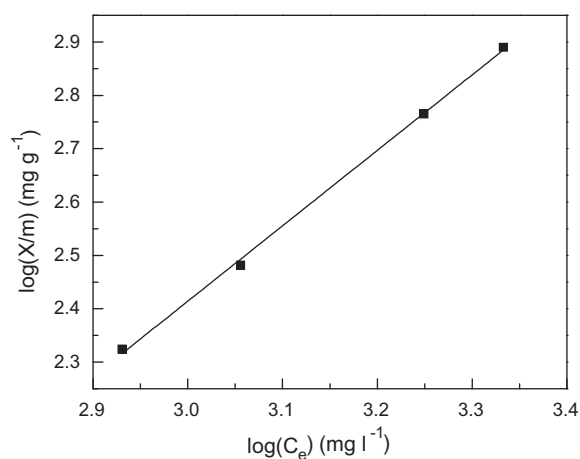
$$q_e = 0.01489 C_e^{1.431} \tag{12}$$

Fig. 12. Freundlich isotherm curve ($EDTA = 0.01\,mol\,l^{-1}$, $pH = 4.35$, $T = 50\,°C$, stirring speed $= 300\,r\,min^{-1}$).

Fig. 13. Plot of $\ln k_2$ vs. $10^3/T$.

Fig. 14. van't Hoff plot for the adsorption of EDTA ($AC = 12.5\,g\,l^{-1}$, pH = 4.25, EDTA = 0.01 mol l^{-1}, $T = 50\,^\circ$C, stirring speed = 300 r min^{-1}).

3.9. Thermodynamic parameters

The second-order rate constant can be expressed as a function of temperature by the Arrhenius equation and the activation energy (E_a) can be determined as below:

$$k_2 = k_0 \exp\left(-\frac{E_a}{RT}\right) \qquad (13)$$

Eq. (13) can be rearranged as follows:

$$\ln k_2 = \ln k_0 - \frac{E_a}{RT} \qquad (14)$$

where k_0 is Arrhenius preexponential factor and E_a is activation energy.

Fig. 13 shows a linear plot of $\ln k_2$ as a function of $10^3/T$ for EDTA adsorption on activated carbon at 313–343 K. The apparent activation energy calculated from the slope of the plot is found to be 6.01 kJ mol^{-1}. The relatively low positive activation energy indicates that physical adsorption dominate the process of EDTA adsorption on to activated carbon.

Thermodynamic parameters, such as change in free energy (ΔG^0), enthalpy (ΔH^0), and entropy (ΔS^0), that describe EDTA uptake by activated carbon can be estimated by considering the equilibrium constants under the several experimental conditions.

Equilibrium constant for the adsorption reaction of EDTA on activated carbon, K_c, is defined as follows:

$$K_c = \frac{C_{AE}}{C_e} = \frac{C_0 - C_e}{C_e} = \frac{C_0}{C_e} - 1 \qquad (15)$$

where C_{AE} is the adsorbed amount of adsorbate at equilibrium, C_0 the initial concentration of adsorbate (mg l^{-1}), and C_e the equilibrium concentration of adsorbate (mg l^{-1}).

The change in the Gibbs free energy for a reaction is expressed as

$$\Delta G^0 = -RT \ln K_c \qquad (16)$$

where R is the gas constant and T is temperature in Kelvin.

Moreover, using the relationship, $\Delta G^0 = \Delta H^0 + T\Delta S^0$, $\ln K_c$ can be expressed in Eq. (17). Thus, if the equilibrium constants for an adsorption reaction at different temperatures are known, the standard enthalpic and entropic changes for adsorption can also be estimated from the slope and intercept of a linear plot of $\ln K_c$ versus $1/T$.

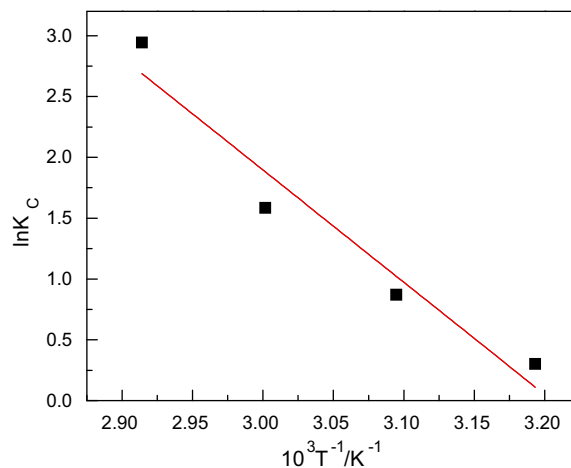$$\ln K_c = \frac{\Delta S^0}{R} - \frac{\Delta H^0}{RT} \qquad (17)$$

Table 3
Thermodynamic parameters of EDTA adsorbed by AC.

	T (K)			
	313	323	333	343
ΔG (kJ mol^{-1})	−0.79	−2.34	−4.39	−8.40
ΔH (kJ mol^{-1})			43.83	
ΔS (J mol^{-1} K^{-1})			141.77	
E_a (kJ mol^{-1})			6.01	

ΔH^0 and ΔS^0 are obtained from the slope and intercept of van't Hoff plot of $\ln K_c$ versus $1/T$ (Fig. 14; Table 3). A positive value of ΔH^0 indicates that the adsorption process is endothermic in nature and negative values of ΔG^0 show the spontaneous adsorption of EDTA on the activated carbon. Positive ΔS^0 shows the increased randomness of the solid/solution interface during the adsorption of EDTA on the activated carbon.

4. Conclusion

In this study, the adsorption of EDTA on activated carbon from aqueous solutions has been studied in a batch stirred cell. The following specific conclusions can be drawn from the experimental results.

1. The impacts of external and internal diffusion on EDTA adsorption on activated carbon could be eliminated with a stirring speed over 300 r min^{-1} and mesh of activated carbon more than 120, respectively.
2. Temperature is advantageous to the adsorption of EDTA on the activated carbon. The values of the EDTA adsorbed at equilibrium (q_e) increase with temperature.
3. The EDTA adsorption on activated carbon increases with its concentration in the aqueous solutions.
4. The EDTA adsorption on per gram of activated carbon decreases as the activated carbon mass increases. But the total adsorptive capability of EDTA increases as the activated carbon mass increases.
5. The EDTA adsorption on activated carbon decreases as the pH value increases.
6. The EDTA adsorption on the activated carbon could be well described by the pseudo-second-order kinetic equation.
7. The Langmuir and Freundlich equilibrium isotherm models are found to provide a good fitting of the adsorption data, with

R^2 0.9920 and 0.9983, respectively. The adsorption capacity of EDTA obtained from the Langmuir equilibrium isotherm model is found to be 1005.05 mg g^{-1}.

8. Thermodynamic parameters such as E_a, ΔG^0, ΔH^0 and ΔS^0 for adsorption reaction are estimated. A positive value of ΔH^0 indicates that the adsorption process is endothermic in nature and negative values of ΔG^0 show the spontaneous adsorption of EDTA on the activated carbon. Positive ΔS^0 shows the increased randomness of the solid/solution interface during the adsorption of EDTA on the activated carbon.

Acknowledgements

References

[1] N.Y. Hishinuma, R. Kaji, H. Akimoto, F. Nakajima, T. Mor, T. Kamo, Y. Arikawa, S. Nozawa, Reversible binding of NO to Fe(II)–EDTA, Bull. Chem. Soc. Jpn. 52 (1979) 2863–2865.

[2] E. Sada, H. Kumazawa, Individual and simultaneous absorption of dilute NO and SO$_2$ in aqueous slurries of MgSO$_3$ with Fe^{II}–EDTA, Ind. Eng. Chem. Process Des. Dev. 19 (1980) 377–382.

[3] S.M. Yih, C.W. Lii, Simultaneous absorption of nitric oxide and sulphur dioxide in Fe^{II}–EDTA solutions in a packed absorber-stripper unit, J. Chem. Eng. 42 (1989) 145–152.

[4] F. Gambardella, J.G.M. Winkelman, H.J. Heeres, Experimental and modelling studies on the simultaneous absorption of NO and O$_2$ in aqueous iron chelate solutions, Chem. Eng. Sci. 61 (2006) 6880–6891.

[5] L. Wang, W.R. Zhao, Z.B. Wu, Simultaneous absorption of NO and SO$_2$ by Fe^{II}–EDTA combined with Na$_2$SO$_3$ solution, J. Chem. Eng. 132 (2007) 227–232.

[6] V. Zang, R. van Eldik, Kinetics and mechanisms of the autoxidation of iron(II) induced through chelation by ethylenediaminetetraacetate and related ligands, Inorg. Chem. 29 (1990) 1705–1711.

[7] H.J. Wubs, A.A.C.M. Beenackers, Kinetics of the oxidation of ferrous chelates of EDTA and HEDTA in aqueous solution, Ind. Eng. Chem. Res. 32 (1993) 2580–2594.

[8] Z.B. Wu, L. Wang, W.R. Zhao, Kinetic study on regeneration of Fe^{II}EDTA in the wet process of NO removal, J. Chem. Eng. 140 (2008) 130–135.

[9] F. Gambardella, L.M.H.J. Heeres, Reactive NO absorption in aqueous Fe^{II}(EDTA) solutions in the presence of denitrifying micro-organisms, J. Chem. Eng. 116 (2006) 67–75.

[10] P. Maas, P. Brink, B. Klapwijk, P. Lens, Acceleration of the Fe(III)EDTA$^-$ reduction rate in BioDeNOx reactors by dosing electron mediating compounds, Chemosphere 7 (2009) 243–249.

[11] I. Manconi, P. Maas, P. Lens, Effect of sulfur compounds on biological reduction of nitric oxide in aqueous Fe(II)EDTA^{2-} solutions, Nitric Oxide 15 (2006) 40–49.

[12] H.S. Zhu, Y.P. Mao, Y. Chen, X.L. Long, W.K. Yuan, Simultaneous absorption of NO and SO$_2$ with Fe^{II}–EDTA solution coupled with the Fe^{II}–EDTA regeneration catalyzed by activated carbon, Sep. Purif. Technol. 74 (2010) 1–6.

[13] X.L. Long, H. Cheng, Z.L. Xin, W.D. Xiao, W. Li, W.K. Yuan, Adsorption of ammonia on activated carbon from aqueous solutions, Environ. Prog. 27 (2008) 225–233.

[14] J.A. Fletcher, Y. Yüzak, K.M. Thomas, Adsorption and desorption kinetics for hydrophilic and hydrophobic vapors on activated carbon, Carbon 44 (2006) 989–1004.

[15] F. Jones, P. Jones, M.I. Ogden, W.R. Richmond, A.L. Rohl, M. Saunders, The interaction of EDTA with barium sulfate, J. Colloid Interface Sci. 316 (2007) 553–561.

[16] E. Repo, T.A. Kurniawan, J.K. Warchol, M.E.T. Sillanpaa, Removal of Co(II) and Ni(II) ions from contaminated water using silica gel functionalized with EDTA and/or DTPA as chelating agents, J. Hazard. Mater. 171 (2009) 1071–1080.

[17] A.R. Bowers, C.P. Huang, Adsorption characteristics of metal–EDTA complexes onto hydrous oxides, J. Colloid Interface Sci. 110 (1986) 575–590.

[18] B. Nowack, J. Luʻtzenkirchen, P. Behra, L. Sigg, Modeling the adsorption of metal–EDTA complexes onto oxides, Environ. Sci. Technol. 30 (1996) 2397–2405.

[19] M.S. Vohra, A.P. Davis, Adsorption of Pb(II), EDTA, and Pb(II)–EDTA onto TiO$_2$, J. Colloid Interface Sci. 198 (1998) 18–26.

[20] D.N. Furlong, D. Wells, W.H.F. Sasse, Colloidal semiconductors in systems for the sacrificial photolysis of water. 1. Preparation of a platinum/titanium dioxide catalyst by heterocoagulation and its physical characterization, J. Phys. Chem. 89 (1985) 626–632.

[21] A.P. Terzyk, Molecular properties and intermolecular forces-factors balancing the effect of carbon surface chemistry in adsorption of organics from dilute aqueous solutions, J. Colloid Interface Sci. 275 (2004) 9–29.

[22] Y.S. Ho, G. McKay, Pseudo-second order model for sorption processes, Process Biochem. 34 (1999) 451–469.

[23] G. McKay, Adsorption of dyestuffs from aqueous solution using activated carbon. III. Intraparticle diffusion processes, J. Chem. Technol. Biotechnol. 33A (1983) 196–204.

[24] H. Moon, W.K. Lee, Intraparticle diffusion in liquid-phase adsorption of phenol with activated carbon in finite batch adsorber, J. Colloid Interface Sci. 96 (1983) 162–170.